Vol 13 No 2, February 2004
1009-1963/2004/13(02)/0243-08

Chinese Physics

© 2004 Chin. Phys. Soc.
and IOP Publishing Ltd

Nonequilibrium dynamical phase transition of 3D kinetic Ising/Heisenberg spin system *

Shao Yuan-Zhi(邵元智)[a)†], Lai J. K. L.[b)], Shek C. H.[b)],
Lin Guang-Ming(林光明)[a)], and Lan Tu(蓝 图)[a)]

[a)] *Department of Physics, Zhongshan University, Guangzhou 510275, China*

[b)] *Department of Physics and Materials Science, City University of Hong Kong, Kowloon, Hong Kong*

(Received 25 February 2003; revised manuscript received 27 May 2003)

We have studied the nonequilibrium dynamic phase transitions of both three-dimensional (3D) kinetic Ising and Heisenberg spin systems in the presence of a perturbative magnetic field by Monte Carlo simulation. The feature of the phase transition is characterized by studying the distribution of the dynamical order parameter. In the case of anisotropic Ising spin system (ISS), the dynamic transition is discontinuous and continuous under low and high temperatures respectively, which indicates the existence of a tri-critical point (TCP) on the phase boundary separating low-temperature order phase and high-temperature disorder phase. The TCP shifts towards the higher temperature region with the decrease of frequency, i.e. $T_{\rm TCP}$=1.33×exp(−ω/30.7). In the case of the isotropic Heisenberg spin system (HSS), however, the situation on dynamic phase transition of HSS is quite different from that of ISS in that no stable dynamical phase transition was observed in kinetic HSS after a threshold time. The evolution of magnetization in the HSS driven by a symmetrical external field after a certain duration always tends asymptotically to a disorder state no matter what an initial state the system starts with. The threshold time τ depends upon the amplitude H_0, reduced temperature $T/T_{\rm C}$ and the frequency ω as $\tau = C \cdot \omega^{\alpha} \cdot H_0^{-\beta} \cdot (T/T_{\rm C})^{-\gamma}$.

Keywords: dynamical phase transition, spin system, Monte Carlo simulation
PACC: 7510, 6470, 7115Q

1. Introduction

Of the classical $O(n)$ spin systems, the situations of n=1 and n=3 stand for two representative cases, namely anisotropic spin-exchange Ising spin system (ISS) and isotropic spin-exchange Heisenberg spin system (HSS).[1,2] Under the action of a time-varying driving field, the $O(n)$ spin system gives rise to various interesting dynamical responses [3,4] among which the most attractive ones are the dynamical phase transition (DPT) and the hysteresis scaling of a spin system.[5−10] Tome and Oliveira [11] first studied the DPT of a kinetic ISS under the action of a sinusoidal alternating magnetic field by solving the mean field dynamical equation of motion and ascertained the dynamical transition phase boundary separating low-temperature order phase and high-temperature disorder phase. Their study also predicated, on the phase boundary line, the existence of a tri-critical point (TCP) across which the nature of dynamical transition changes between continuous to discontinuous.[11] However, their approach, based on the solution to the mean field dynamical equation of motion without the consideration of noise or fluctuation, did not tackle the real cases of dynamic transition. Lo and Pelcovits [12] computed the dynamical transition of a two-dimensional (2D) kinetic ISS by Monte Carlo (MC) simulation which itself incorporates the effect of fluctuations. Unfortunately, their work did not give any precise phase boundary of the dynamical transition. In the early work of Acharyya *et al*,[5] the dynamical transition of a kinetic ISS (1D–4D) was studied systematically, and the dynamical transition boundary lines were drawn on the plane of external field amplitude with the temperature as well as the relevant TCPs located generally on the transition boundary lines. Their results of MC simulation in a large temperature range from 0 to 8, however, made it imperfect

*Project supported by the Scientific Research Fund of Guangdong Province, China (Grant No 021693) and the Research Grants Council of Hong Kong, China (Project No City U 1022/98E).

†E-mail: stssyz@zsu.edu.cn

to exhibit the delicate trend of the DPT within the small but more interesting temperature range from 0 to 1. Their results also fail to present the effect of frequency on the location of TCP. Through studying the statistical distribution of the dynamical order parameter and the temperature variation of the fourth-order Binder cumulant, Acharyya [13] further investigated accurately the influence of temperature on the dynamical transition of a 2D kinetic ISS while keeping both the amplitude and the frequency of the driving field fixed. To identify quantitatively the nature of critical dynamical transition occurring to a kinetic Ising model under the application of an oscillating field, Sides *et al* [4,14] recently applied the finite-size scaling theory to a 2D ISS and figured out the critical frequency and the critical exponents of the relevant system precisely. Generally, the understanding of the DPT feature of a 3D ISS (HSS) remains scarce in comparison with that of a 2D ISS.

Motivated by our ongoing research on the magnetism of bulk amorphous/nano-crystalline materials [15,16] as well as our previous relevant MC simulations,[10,17−20] we focus in this paper on the DPT nature of a 3D anisotropic ISS and an isotropic HSS. Firstly, we study the relationship of the system response of a kinetic 3D ISS to the amplitude of the external field by holding temperature and the frequency fixed. Furthermore, we precisely draw the phase boundary of the DPT within the temperature range from 0 to 1, and then ascertain accurately the TCP position on the boundary line as well as the variation of the TCP position along the phase boundary line while the frequency alters. In addition, the DPT of a 3D HSS is studied, which demonstrates a feature significantly dissimilar to that of a 3D ISS. To our best knowledge, there has not yet been such a study on 3D HSS reported so far.

2. Descriptions of model and computational algorithm

2.1. Model and other simulation parameters

The Hamiltonian of a classical $O(n)$ spin system driven by a uniaxial anisotropic external field H parallel to the z-axis can be written in the form as shown in Eq.(1a),

$$\hat{H} = -(J_{\rm NN} + J_{\rm NNN}) \sum_{<i,j>} (\boldsymbol{S}_i \cdot \boldsymbol{S}_j) - g\mu \sum_i (\boldsymbol{H} \cdot \boldsymbol{S}_j), \tag{1a}$$

where

$$\boldsymbol{S}_i \cdot \boldsymbol{S}_j = aS_i^x S_j^x + bS_i^y S_j^y + cS_i^z S_j^z. \tag{1b}$$

There are two types of energy terms in the components of the Hamiltonian. They are the spin exchange energy and the interacting energy between the spin and the driving field. S_i and S_j in the equation represent the spins at sites i and j, respectively, within the lattice. S^x, S^y and S^z in Eq.(1b) denote, in turn, the projections of spin S along the x-, y- and z-axes. The spin-exchange constants $J_{\rm NN}$ and $J_{\rm NNN}$ signify the interaction of site i with its nearest neighbours (NN) and with its next-nearest neighbour (NNN) respectively. Depending on whether $J_{\rm NN}$ or $J_{\rm NNN}$ is considered, the summation $\sum_{<i,j>}$ symbolizes the sum over NN or NNN site pairs, respectively. Parameters a, b and c, ranging from 0 to 1, are anisotropy constants of spin exchange. The isotropic HSS corresponds to the case when $a = b = c$=1. On the other hand, if $a = b$=0 and c=1 the Hamiltonian describes the anisotropic ISS. The ratio between the critical temperature and the exchange interaction, $kT_{\rm c}/J_{\rm NN}$, is calculated using Eq.(2),[21],

$$kT_{\rm c}/J_{\rm NN} = 5(R-1)[11S(S+1)-1]/96, \tag{2}$$

where R, S, k and $T_{\rm c}$ are the number of nearest neighbours, lattice spin, Boltzmann constant and critical temperature respectively. The interaction between site i with the next-nearest neighbour $J_{\rm NNN}$, which drops exponentially with respect to the distance between lattice sites,[22] can be determined from $J_{\rm NN}$ and is usually taken to be 0.10−−0.25 $J_{\rm NN}$.[23] In this paper, we take $J_{\rm NNN}$ to be 0.2 $J_{\rm NN}$.

2.2. Algorithm of MC simulation

In MC simulations the orientations of the lattice spins can be initialized either orderly, such that all lattice spins align parallel to the z-axis, or randomly. We employed random initialization to evade the influence of retained order on the final results. Periodic boundary condition was used to minimize the influence of the finite lattice size. The spherical coordinate system was adopted with symbols ψ and θ signifying the azimuthal angle of the final average moment and the angle the final average moment made with the z-axis respectively. A lattice site i with spin orientation $S_i(\theta_i, \psi_i)$ was chosen randomly and the value of the Hamiltonian was calculated with Eq.(1) as H_i. The spin on this lattice site was then rotated to a new random orientation, $S_{\rm n}(\theta_{\rm n}, \psi_{\rm n})$ and the new value of the

Hamiltonian H_n of site i was similarly calculated with Eq.(1). The energy variation caused by such a change of spin orientation is

$$\Delta H = H_n - H_i. \tag{3a}$$

The Metropolis criterion [24] was adopted to determine whether the new spin orientation is adopted or rejected. The energy change must satisfy the condition below for a successful spin orientation change,

$$\exp[-\Delta H/kT] \geq P \in (0,1), \tag{3b}$$

where P is a random number within the range from 0 to 1.

The simulation proceeded by sweeping every lattice site in sequence for a number of repetitions (Monte Carlo steps, MCSs) and the statistical averages of the magnetic properties concerned were computed over ten independent simulations. Standard tests were performed to verify whether equilibrium under the prescribed condition was attained. All simulations were performed on a three-dimensional lattice with a periodic boundary condition and lattice size N=60−100. In our simulation the sweeping times were counted up to 10^5 MCSs.

2.3. Magnetic properties concerned in this paper

In our simulation, we kept the spin system in contact with an isothermal heat bath at temperature T and applied a sinusoidally driving field $H(t)$ parallel to the z-axis:

$$H(t) = H_0 \cdot \sin(\omega t). \tag{4}$$

Here H_0 and ω ($=2\pi f$) in the equation are the amplitude and the angular frequency, respectively, of the oscillating external field. With $\boldsymbol{S}_i$ denoting the magnetic spin occupying site i at time t, the instantaneous magnetization $m(t)$ averaged over all lattice sites is given by

$$m(t) = \frac{1}{N^3}\sum_i \boldsymbol{S}_i. \tag{5}$$

The dynamical order parameter Q is defined as the statistical average of the instantaneous magnetization $m(t)$ over a complete period τ of the oscillating external field.

$$Q = \frac{1}{\tau}\oint m(t)\mathrm{d}t. \tag{6}$$

For a disorder state, the instantaneous magnetization $m(t)$ is symmetric about the time axis in a complete period τ of the oscillating field if Q=0. On the contrary, $m(t)$ becomes asymmetric if $Q \neq 0$, which represents an order state due to the appearance of symmetry-breaking. The DPT is associated with the breaking of the symmetry of the dynamical hysteresis loop. For a dynamically disordered phase the value of the order parameter vanishes (Q=0) and the corresponding hysteresis loop is symmetric. In the dynamically ordered phase which exhibits a nonzero order parameter ($Q \neq 0$), the hysteresis loop loses its symmetry. Keeping the frequency fixed, we have computed the Q parameter and its statistical distribution $P(Q)$ under the various combinations of temperatures and amplitudes of the driving field. The nature of the DPT is revealed directly from the features of the $P(Q)$ distribution. Moreover, the influence of varying frequency on the DPT was also taken into account.

3. Results

3.1. The DPT in an ISS

In order to compute the Q parameter and its statistical distribution $P(Q)$, it is necessary to determine the variation of magnetization $m(t)$ against time t. Figure 1 shows the partial curves of $m(t)$ versus t in three typical external field amplitudes at a reduced temperature T/T_c=0.4 and angular frequency ω=32. The larger amplitude (H_0=2.40) results in the symmetric variation of magnetization $m(t)$ with time t as displayed in Fig.1(a). Moreover, in this symmetric case the Q parameter takes a zero value. The smaller amplitude (H_0=2.02) leads to an asymmetric trend of $m(t)$–t as shown in Fig.1(b). The $m(t)$ value oscillates slightly around m=0.8, and $m(t)$ remains positive under the alternating driving field. The Q parameter is non-zero in this situation, giving rise to the breaking of symmetry. In most cases with intermediate amplitudes such as that for H_0=2.18 in Fig.1(c), however, the $m(t)$–t curve becomes aperiodic. The Q parameter is zero in some periods but non-zero in others as shown in Fig.1(c). Therefore, it is necessary to make a thorough assessment of the Q parameter by calculating its statistical distribution $P(Q)$.

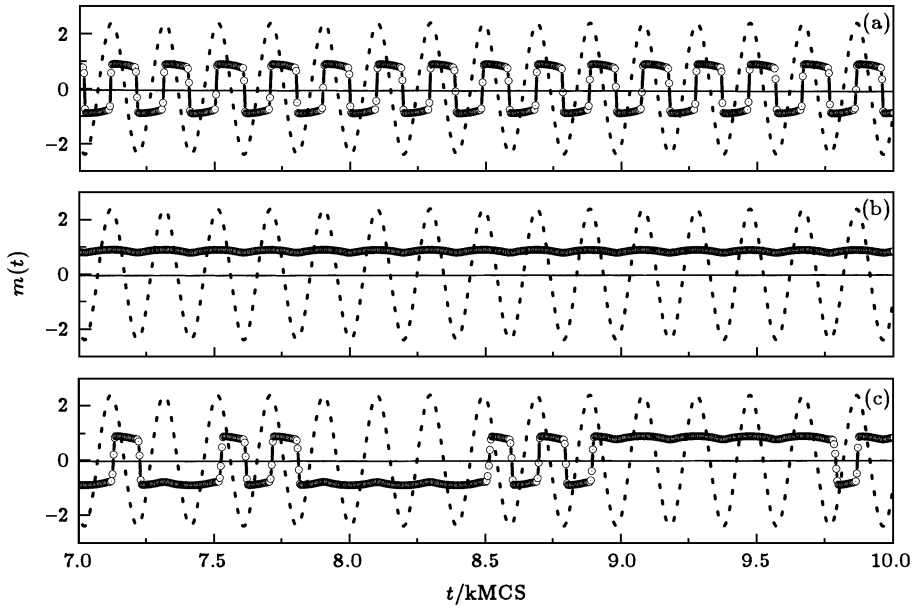


Fig.1. The evolution of both magnetization (circle) and driving field (dotted curve) at a reduced temperature T/T_c=0.4, with fixed frequency ω=32 but different amplitudes of the driving field H_0. (a) H_0=2.40, (b) H_0=2.02 and (c) H_0=2.18.

Based on the study of the statistical distribution of Q parameter $P(Q)$, we have further determined the DPT boundary of the system at different frequencies. The ratio λ of the number of periods for Q=0 to that for $Q \neq 0$ was calculated for different amplitudes H_0. The moment when λ changes from less than 0.5 to larger than 0.5 is usually regarded as the onset of the DPT from an ordered phase to disordered phase, and the value of H_0 is defined as the critical amplitude H_{0c}. The trace of these H_{0c} points on the H_0-(T/T_c) plane represents the DPT boundary as shown in Fig.2. The states located at below and above the phase boundary correspond to a low-temperature ordered phase ($Q \neq 0$) with symmetry-breaking and a high-temperature disordered phase without symmetry-breaking (Q=0), respectively. It could be seen from Fig.2 that the critical amplitude H_{0c} of the driving field at which the DPT occurs declines monotonically with reduced temperature T/T_c and that the delicate effect of frequency on the phase boundary is negligible.

As expounded above, the Q parameter always

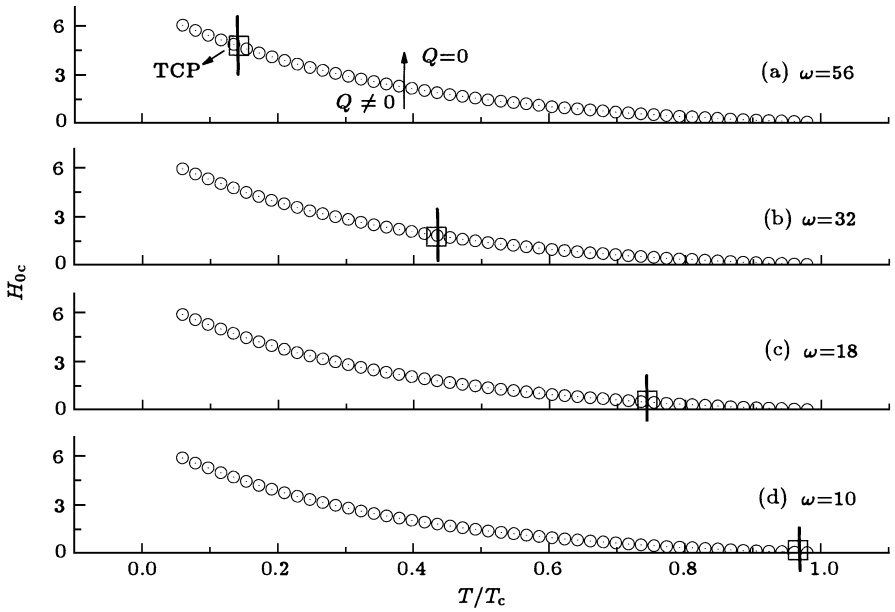


Fig.2. Dynamical transition boundary separating ordered ($Q \neq 0$) and disordered (Q=0) phases under various frequencies of the driving field ω. (a) ω=56, (b) ω=32, (c) ω=18, (d) ω=10. Square symbols on the boundary signify the positions of tri-critical point (TCP).

changes from nonzero to zero with the increase of amplitude of the driving field. In order to locate the TCP position on the phase boundary accurately, we compute the $P(Q)$ of numerous states in the vicinity of the phase boundary as well as the dependence of $P(Q)$ on the reduced temperature. Figure 3(a) displays the $P(Q)$ values of the system at low temperature T/T_c=0.1 with five different amplitudes, H_0. The increase of amplitude causes an abrupt decrease of $P(Q)$ from Q=0.9 to Q=0 without any intermediate states, characterizing the discontinuous dynamic transition of the system. In the case of higher temperature like T/T_c=0.7 and the same five amplitudes as before, the increase of amplitude results in a gradual decline of $P(Q)$ with the appearance of obvious intermediate states as displayed in Fig.3(b). Evidently, continuous dynamic transition takes place in this situation. We have ascertained the TCP from the phase boundary above by finding out the point at which the boundary of discontinuous transition intersects that of continuous transition, and we mark the TCPs of different frequencies on the phase boundaries in Fig.2. The temperature at TCP is referred to as the tri-critical temperature $T_{\rm TCP}$ and the regions of $T < T_{\rm TCP}$ and $T > T_{\rm TCP}$ correspond to the discontinuous and continuous transition respectively.

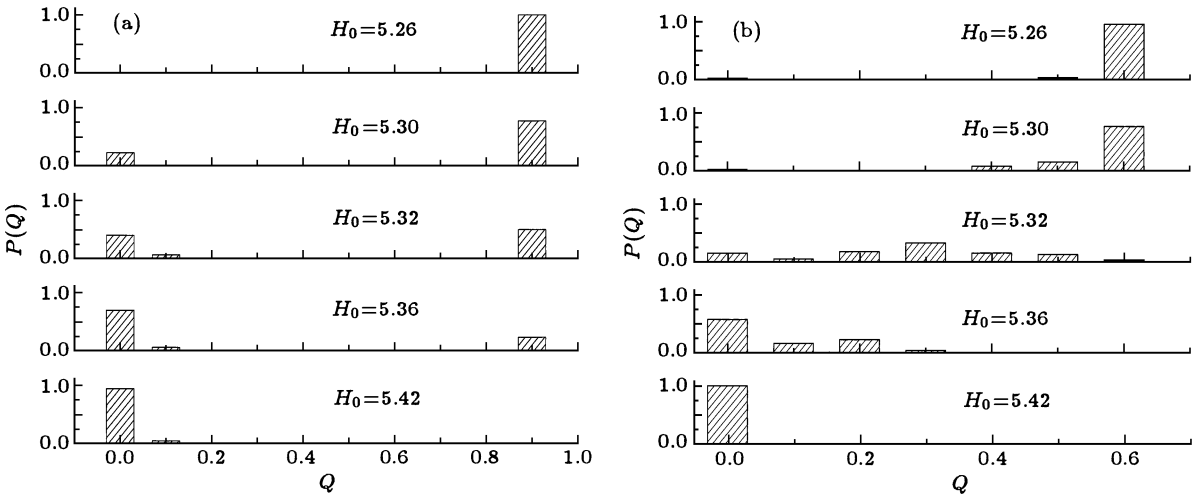


Fig.3. Histogram of statistical distribution of dynamical order parameter Q with different reduced temperature as well as frequency and amplitude of driving field. (a) ω=10, T/T_c=0.1; (b) ω=100, T/T_c=0.7.

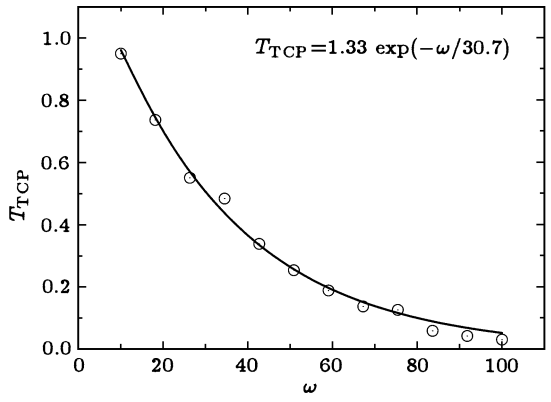


Fig.4. The tri-critical temperature $T_{\rm TCP}$ versus the frequency ω.

The frequency affects the TCPs drastically though this only modifies the phase boundary negligibly. As shown in Fig.2, the TCPs shift to the high-temperature region while the frequency of driving field reduces, and this indicates the enlargement of the discontinuous transition region. We plotted the tri-critical temperature $T_{\rm TCP}$ against the frequency ω in Fig.4. An exponential relationship between $T_{\rm TCP}$ and ω is established empirically by curve-fitting, $T_{\rm TCP}$=1.33×exp(−ω/30.7).

3.2. The DPT in the HSS

For the isotropic 3D HSS, its behaviour in dynamical transition is quite different from that of the anisotropic 3D ISS. No real stable ordered state and relevant DPT can be observed in our numerical simulations to the kinetic HSS. The evolution of magnetization $m(t)$ in the HSS driven by a symmetrical external field after a certain duration denoted by the threshold time always tends asymptotically to a disorder state regardless of the initial state of the system.

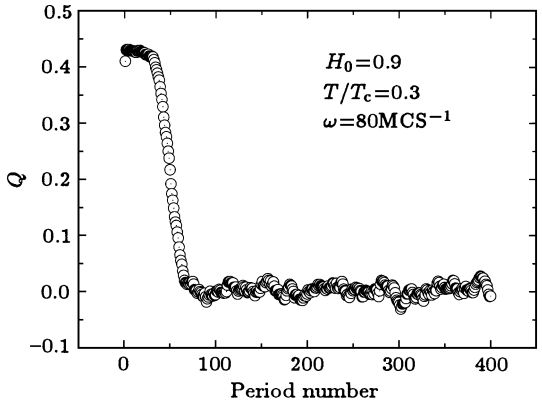


Fig.5. The Q parameter versus the number of periods of the driving field.

Figure 5 presents a typical curve of the dynamical order parameter Q of the HSS versus time. We performed many simulations for the HSS in wide ranges of reduced temperature ($0.1 \leq T/T_c \leq 0.9$), frequency ($1 \leq \omega \leq 160$) and amplitude ($0.05 \leq H_0 \leq 2.0$). A trend similar to that exhibited in Fig.5 can always be observed no matter what combination of the parameters is used. There exists a threshold time τ after which the dynamic order parameter Q becomes zero. The threshold time is controlled by temperature as well as the frequency and the amplitude of the driving field. In Fig.6 we plot the curves of the threshold time τ versus the amplitude H_0, reduced temperature T/T_c and frequency ω, respectively. The threshold time τ shown in the figure is expressed in terms of the number of periods of the driving field. Evidently, the threshold time τ decays with the increase of both the amplitude and reduced temperature, but grows with increasing frequency. By means of multiple regression, we establish the formula relating the threshold time τ with the amplitude H_0, reduced temperature T/T_c and the frequency ω as follows:

$$\tau = C \cdot \omega^{\alpha} \cdot H_0^{-\beta} \cdot (T/T_c)^{-\gamma}, \qquad (7)$$

where C is a constant equal to 0.0302 for our lattice, exponents α=1.18±0.01, β=1.81±0.01 and γ=1.68±0.01, respectively.

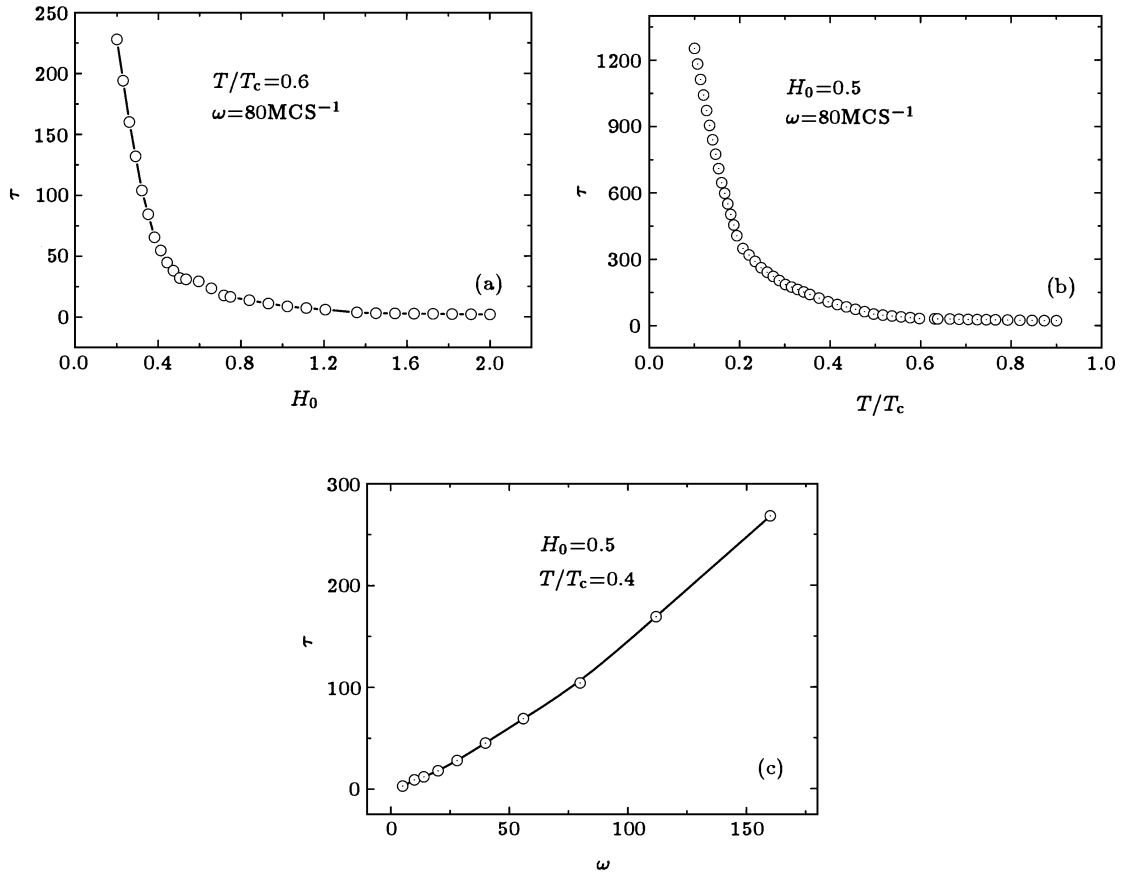


Fig.6. The curves of τ-H_0 (a), τ-T/T_c (b) and τ-ω (c).

4. Discussion

Two types of competing time scales, namely the relaxation time of the system and the period of the applied field, dominate the response of a spin system under an external field. When the spin system is driven by an oscillating magnetic field, the magnetic system usually cannot respond instantaneously owing to the relaxation delay. The system therefore gains dynamical hysteresis because the magnetization lags behind the applied field. When the period of the driving field is much shorter than the relaxation time of the system, the hysteresis loop becomes asymmetric around the origin and the DPT occurs spontaneously out of dynamic symmetry-breaking, i.e. nonvanishing Q parameter.

In addition to the frequency ω, the amplitude H_0 also has an apparent effect on the DPT. Under a larger field H_0, the relaxational time of the system for spin-flip becomes short compared with the period of the driving field, and the magnetization can follow the symmetric feature, though with a certain phase difference, of the driving field as shown in Fig.1(a). The system exhibits a symmetric hysteresis loop with Q=0. On the other hand, when H_0 is small, the relaxation time for spin-flip is much longer than the period of the driving field, and the magnetization cannot keep pace with the oscillating field. The magnetization simply remains in a state of either $m(t) > 0$ or $m(t) < 0$ (depending upon the initial state), as shown in Fig.1(b). Evidently, the Q parameter is nonzero in this situation, implying the presence of an ordered phase with an asymmetric hysteresis loop. The DPT takes place while the Q parameter changes from zero to nonzero. In the case of intermediate amplitude as in Fig.1(c), the magnetization varies in an aperiodic way or oscillates with a very long period. The Q parameter equals zero in some range of time, and nonzero (either $Q > 0$ or $Q < 0$) in the other range with a certain statistical distribution $P(Q)$. The instantaneous magnetization $m(t)$ can either stay at one of the metastable (or stable) states, or simply jump among them randomly because of thermal fluctuations. It is also not difficult to interpret the effect of the amplitude H_0 on the symmetry of hysteresis loop from the mean-field theory. The mean-field approximation indicates that it is impossible to obtain a symmetric hysteresis loop when the amplitude H_0 is smaller than the spinodal field $H_{\rm sp}$. Hysteretic behaviour is observed only when the amplitude H_0 reaches a value $H_{\rm m}$ which is larger than $H_{\rm sp}$ and $H_{\rm m}$ is a monotonically increasing function of the frequency ω.[7]

From Fig.2 one can see that the critical amplitudes H_{0c}, i.e. DPT boundary, diminish with increasing reduced temperature, and a higher temperature facilitates the DPT in smaller amplitude of the driving field. Within the range of reduced temperature from 0 to 1, the DPT boundary displays essentially a little difference even though the frequency alters noticeably. This is similar to what Acharyya *et al* found in Ising model while the temperature is below one.[5] The TCP, nevertheless, alters obviously with the frequency exponentially. The shift of $T_{\rm TCP}$ to a high temperature at low frequency means that the region originally exhibiting continuous transition at high frequency changes into one in which discontinuous transition occurs. Generally speaking, discontinuous transition takes place easily at low temperature and low frequency, and continuous one occurs at high temperature and high frequency.

Unlike the DPT that occurs in anisotropic ISS, the isotropic HSS responses distinctively different to an alternating field. No stable DPT was observed in a kinetic HSS after a threshold time. The evolution of Q parameter in the HSS driven by a symmetrical external field after the threshold time always tends asymptotically to a disorder state no matter what the initial state the system starts with. Owing to the fully isotropic spin-exchange in the HSS, the spins do not take any preferential orientations in the absence of an external field. The magnetic moments, unless driven by either an asymmetric field or a symmetric field with a very large frequency, can closely follow the driving field and give rise to a symmetric hysteresis loop with Q vanished. Thus, the initial symmetry-breaking of the system disappears finally after the threshold time. When the frequency increases largely, however, the magnetic moments cannot follow the oscillation of the driving field easily due to the intrinsic relaxation delay of an interacting spin system. The threshold time, therefore, grows with the frequency and this is exactly what we observed in our simulation. It is not difficult to understand that the threshold time declines with increasing amplitude and temperature because large amplitude keeps the moments in phase with the driving field more easily. Thermal agitation at high temperatures speeds up the dynamic of spin-flip and results in prompt responses of the spins to the driving field.

5. Conclusions

We have studied the nonequilibrium DPT of 3D kinetic ISS and HSS by means of MC simulation. For the anisotropic ISS, its boundary of DPT can be determined accurately by computation. The states above and below the boundary correspond to the high-temperature disordered phase and low-temperature ordered phase respectively. The influence of the driving field frequency on the DPT boundary is weak within the temperature range from 0 to 1. On the DPT boundary there is a TCP at which the discontinuous transition and continuous transition coexist dynamically. The location of the TCP, $T_{\rm TCP}$, depends strongly on the frequency ω of the driving field, and they are related by the equation, $T_{\rm TCP} = 1.33\times \exp(-\omega/30.7)$.

For the isotropic HSS, its behaviours in dynamical transition are significantly different from those of the anisotropic ISS. No real stable ordered state and relevant DPT were observed in our numerical simulations to the kinetic HSS. There exists a threshold time τ after which the magnetization $m(t)$ in the HSS driven by a symmetrical external field always tends asymptotically to a disorder state regardless of the initial state of the system. The threshold time τ depends on the reduced temperature $T/T_{\rm c}$ as well as the amplitude H_0 and the frequency ω of the external field in the form $\tau = C\omega^{\alpha} H_0^{-\beta}(T/T_{\rm c})^{-\gamma}$. C is a constant equal to 0.0302 for our lattice and exponents $\alpha = 1.18\pm0.01$, $\beta = 1.81\pm0.01$ and $\gamma = 1.68\pm0.01$, respectively.

References

[1] Hoffmann K H and Schreiber M 1996 *Computational Physics* (Berlin: Springer) p10

[2] Ausloos M and Elliot R J 1983 *Magnetic Phase Transitions* (Berlin: Springer) p46

[3] Chakrabarti B K and Acharyya M 1999 *Rev. Mod. Phys.* **71** 847

[4] Sides S W, Rikvold P A and Novotny M A 1998 *Phys. Rev.* E **57** 6512

[5] Acharyya M and Chakrabarti B K 1995 *Phys. Rev.* B **52** 6550

[6] Acharyya M 1998 *Phys. Rev.* E **58** 174

[7] Rao M, Krishnamurthy H R and Pandit R 1990 *Phys. Rev.* B **42** 856

[8] Sides S W, Ramos R A and Rikvold P A 1997 *J. Appl. Phys.* **81** 5597

[9] He Y L and Wang G C 1993 *Phys. Rev. Lett.* **70** 2336

[10] Shao Y Z, Shek C H and Lai J K 1999 *Phys. Stat. Sol.* B **214** R11

[11] Tome T and Oliveira M J 1990 *Phys. Rev.* A **41** 4251

[12] Lo W S and Pelcovits R A 1990 *Phys. Rev.* A **42** 7471

[13] Acharyya M 1999 *Phys. Rev.* E **59** 218

[14] Sides S W, Rikvold P A and Novotny M A 1998 *Phys. Rev. Lett.* **81** 834

[15] Shao Y Z, Lan T and Lin G M 2001 *Chin. J. Nonferr. Met.* **11** 362 (in Chinese)

[16] Shao Y Z, Lin G M, Lan T and Zhong W R 2002 *Acta Phys. Sin.* **51** 2362 (in Chinese)

[17] Shao Y Z, Lan T and Lin G M 2001 *Acta Phys. Sin.* **50** 942 (in Chinese)

[18] Shao Y Z, Lan T and Lin G M 2001 *Acta Phys. Sin.* **50** 948 (in Chinese)

[19] Shao Y Z, Lai J K, Shek C H, Lin G M and Lan T 2002 *Phys. Stat. Sol.* B **232** 330

[20] Shek C H, Shao Y Z and Lai J K 2000 *Physica* A **276** 201

[21] Rushbrooke G S and Wood P J 1958 *Mol. Phys.* **1** 257

[22] Wagner D 1972 *Introduction to the Theory of Magnetism* (New York: Pergamon) p153

[23] Mlodzki J, Wuensch F R and Galazka R R 1990 *J. Magn. Magn. Mater.* **86** 269

[24] Binder K and Heermann D W 1992 *Monte Carlo Simulation in Statistical Physics* (Berlin: Springer) p14